J Therm Anal Calorim (2010) 101:695–699
DOI 10.1007/s10973-010-0914-6

Thermal analysis of kidney stones and their characterization

A. Kohutova · P. Honcova · V. Podzemna ·
P. Bezdicka · E. Vecernikova ·
M. Louda · J. Seidel

CCTA10 Special Issue

Abstract Thermal decomposition and structural characterization of three human kidney stones (KS1–KS3) extracted from patients of Eastern Bohemia have been carried out using X-ray powder diffraction systems (XRD), scanning electron microscope with energy dispersive X-ray micro analyser (SEM-EDX) and differential thermal analysis (DTA). The samples KS1 and KS2 solely consisted of calcium oxalate monohydrate (a.k.a. whewellite, $CaC_2O_4{\cdot}H_2O$). The third sample, KS3, was formed from calcium oxalate dihydrate (weddellite, $CaC_2O_4{\cdot}2H_2O$), calcium oxalate monohydrate, and hydroxyapatite (HA, $Ca_{10}(PO_4)_6(OH)_2$). Thermal measurements were carried out in the range between room temperature and 1,230 °C. XRD analysis was utilized to investigate the change of phases at 800 and 1,230 °C.

Keywords Kidney stones · Characterization · Thermal analysis · Decomposition

Introduction

Kidney stones are hard, solid products that form in the urinary tract. General conditions that contribute to stone formation include, e.g., a high concentration of salts in urine, retention of these salts and crystals, pH, infection, and a decrease in the body's natural inhibitors of crystal formation. Calculi are often heterogeneous, containing mainly oxalate, phosphate, and uric acid crystals. The sequence of events that triggers stone formation is not fully understood yet.

Urinary stones are located in the kidneys, and only a small percentage is lodged in the urinary bladder and urethra. The composition of kidney stones can be classified into two parts. The first part is represented by organic matrix containing mainly proteins, lipids, carbohydrates, and cellular components. The other part is biomineral component. There are three main types of kidney stones, according to the occurrence of biominerals [1]: oxalate stones which contain salts of oxalic acid; phosphates stones which contain salts of orthophosphoric acid; and urate stones which mostly consist of uric acid and its salts. Table 1 shows the percentage occurrence of the stones according to abundance. Other, minor phases in urolithiasis are, e.g., cystine, xanthine, calcium carbonate, silicon dioxide, or calcium sulfate dihydrate.

Several factors are responsible for the formation of urolithiasis. The understanding of these processes is important for the treatment and prevention of urinary stones. In general, conditions that contribute to stone formation include mainly dietary preferences, water quality, climate, genetics, disorders, and metabolic imbalance. These conditions have been cited for the high prevalence of kidney stones disease in some countries, but no consensus has been reached [2]. The causes lead to an increase of salt concentration, retention, and their crystallization in urine.

A. Kohutova (✉) · P. Honcova · V. Podzemna
Department of Inorganic Technology, University of Pardubice,
Cs. Legion's Sq. 565, 532 10 Pardubice, Czech Republic
e-mail: anna.kohutova@student.upce.cz

P. Bezdicka · E. Vecernikova
Institute of Inorganic Chemistry, Acad. Sci. CR,
25068 Rez u Prahy, Czech Republic

M. Louda
Department of Urology, University Hospital and Faculty
of Medicine Charles University in Hradec Kralove,
50038 Hradec Kralove, Czech Republic

J. Seidel
Department of Physical Chemistry, TU Bergakademie Freiberg,
Leipziger Str. 29, 09596 Freiberg, Germany

Table 1 Mineral structure of the kidney stones and their occurrence

Composition	Occurrence/%
Whewellite ($CaC_2O_4 \cdot H_2O$)	40–60
Weddellite ($CaC_2O_4 \cdot 2H_2O$)	40–60
Calcium phosphates	20–50
Calcium oxalate + calcium phosphate	35–40
Struvite ($NH_4MgPO_4 \cdot 6H_2O$)	5–15
Uric acid	5–10
Uric acid + urate	~9
Calcium oxalate + urate	~8
Calcium oxalate + uric acid	4–7
Urates	0.2–1

Analytical methods such as chemical analysis, optical and electron microscopy, infrared spectroscopy with Fourier transformation (FTIR), Raman spectroscopy, X-ray powder diffraction, NMR method, and thermal analysis are generally used for qualitative and quantitative classification of urinary calculi. A combination of these methods provides information about stone composition. It should enable more reliable and efficient treatment of individual patients to prevent recurrence of stones.

The thermal decomposition and structural study of biological materials—urinary calculi [3–5], enamel and dentin [6], and bones [7–9]—have been studied many times. The thermal study of kidney stones has been published [10, 11]. In this study, we report some thermal analysis studies of kidney stones and also study the structural changes of kidney stones through thermal decomposition.

This study is focused on examination of components in acquired samples and their possible transformation in solid state. The data provided by this study are helpful for the further study of heterogeneous systems in aqueous solution.

Materials and methods

Samples

Three kidney stones used in this study were obtained from the urology unit of the Hospital Hradec Kralove. The calculi were cleaned using surgical alcohol to remove any blood clots, washed with distilled water, and dried at room temperature. Each sample was cut into two parts. The first part, which was powdered separately in an agate mortar, was investigated by X-ray diffraction and thermal analysis. The second part, so-called cross-cut samples, was observed by microscope.

Structure analysis

Techniques used for the phase analysis are (1) X-ray powder diffraction systems and (2) scanning electron microscope with energy dispersive X-ray spectrometer (EDS). In the first case, the samples were used in powder form, and in the latter case as cross-cut samples.

Crystallinity and phase composition of the kidney stones were studied via XRD. The measurement was realized by diffractometer PANalytical X'PertPRO with Co K_α X-ray tube ($U = 40$ kV, $I = 30$ mA) and Fe β-filter. Qualitative analysis was performed using HighScore software package (PANalytical, The Netherlands, version 1.0d). Diffrac-Plus software package (Bruker AXS, Germany, version 8.0), and JCPDS PDF-2 database [12].

The SEM-EDS, using Jeol JSM-5500 LV apparatus equipped with analyser IXRF Systems and detector Gresham Sirius 10, studied composition and chemical heterogeneity. Accuracy of EDS analysis is better than ±0.5 at.%. Accelerating voltage U = 20 kV, SE signal, high vacuum mode were applied.

Thermal study

Calorimetric and micro gravimetric measurements were carried out by means of the simultaneous thermal analysis NETZSCH STA 409. The calorimeter was coupled to mass spectrometer QMS 403/4 (Balzers) for gas analysis. Only selected gases were analysed in regime MID (multiple ion detection) for mass 18 and 44.

Approximately 3.7 mg of sample, and reference substance (α-Al_2O_3, Merck) were heated (the rate 5 °C/min) in a temperature range from room temperature to 1,230 °C in a flowing argon atmosphere (75 cm^3/min). Crucibles (0.1 mL) and thermocouples were of platinum. X-ray diffraction was used to investigate the change of crystalline phases at 800 and 1,230 °C.

Results and discussion

Structural and microstructural analysis

The powdered samples were analyzed by XRD before thermal analysis. The samples KS1 and KS2 contain only calcium oxalate monohydrate. The sample KS3 contains calcium oxalate monohydrate (33 wt%) as well, and "in addition" hydroxyapatite (11 wt%) and calcium oxalate dihydrate (56 wt%) as major phase. Thermal behaviour of samples of kidney stones was observed at higher temperature.

The cross-cut samples were analyzed by EDS microanalysis (Fig. 1). The zones indicate structural and colour

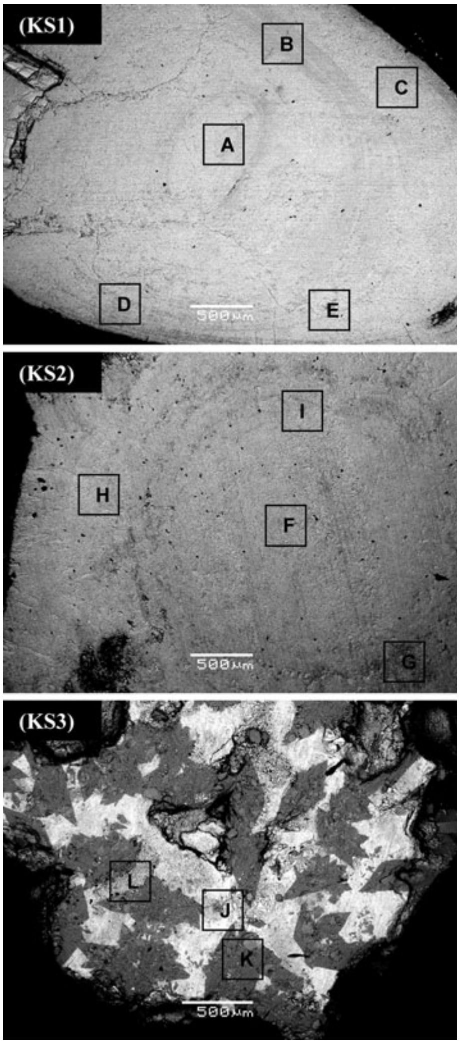

Fig. 1 Structural details of the cross-cut samples

Table 2 EDS result from the cross-cut samples

Sample	Zone	Compositions/at.%						
		O	P	Ca	Si	Na	Mg	Cl
KS1	A	83.15	0.25	16.60	–	–	–	–
	B	82.92	0.23	16.44	0.40	–	–	–
	C	83.01	0.25	16.59	0.15	–	–	–
	D	86.46	0.47	12.89	0.18	–	–	–
	E	69.93	11.23	17.19	0.70	0.60	0.24	0.12
KS2	F	83.41	0.26	15.96	0.37			
	G	83.23	0.20	15.78	0.80			
	H	85.46	0.24	13.83	0.46			
	I	85.90	–	13.31	0.79			
KS3	J	70.27	11.92	16.29	0.14	0.92	0.34	0.12
	K	73.70	10.11	15.13	–	0.88	–	0.18
	L	83.75	1.03	15.22	–	–	–	–

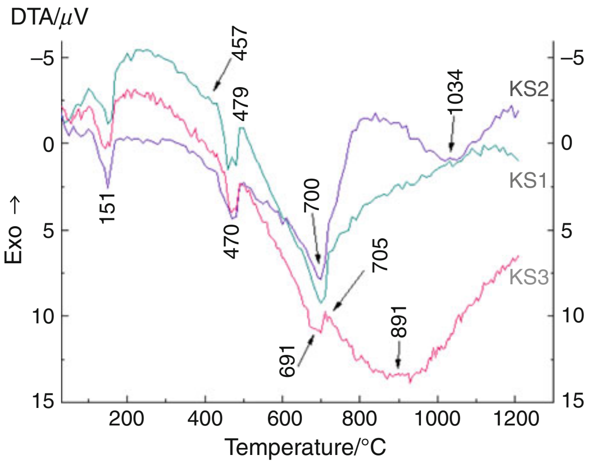

Fig. 2 DTA curves of the powdered samples KS1–KS3

differences, which generally correspond to variable chemical element content, as seen in the Table 2. The samples KS1 and KS2 suggest a relatively similar structure. They both contain mainly oxygen and calcium, and small amounts of phosphorus and silicon. Zone E in sample KS1 indicates the occurrence of magnesium that is probably in a phosphate form. However, XRD technique confirmed the presence of only one phase, i.e., calcium oxalate monohydrate. Their compositions are relatively homogeneous from the nucleus (central part) to the periphery with random impurities. Different rates of crystallization produce colour dissimilarities of zones in kidney stones. The sample KS3 differs from the previous two samples. Its structure is formed by three zones—J, K and L—and the nucleus is not indicated. Zones J and K contain significant amount of phosphorus. X-ray powder diffraction confirmed the presence of three phases: whewellite ($CaC_2O_4{\cdot}H_2O$), weddelite ($CaC_2O_4{\cdot}2H_2O$) and hydroxyapatite ($Ca_{10}(PO_4)_6(OH)_2$).

Thermal studies

The curves of calculi were compared (Fig. 2). The differences between weight loss and shapes of the curves might be attributed to the natural origin of the kidney stones. The curves of all the samples show three, relatively identical regions of weight loss up to 700 °C. The first gradual weight loss with an endothermic process (up to 200 °C) is due to liberation of the coordinated water molecule in whewellite (KS1 and KS2) or its mixture with weddelite (KS3), as major phase. The second region of weight loss (~470 °C) is a superposition of two peaks. These peaks are due to conversion of anhydrous calcium oxalate into calcium carbonate with a release of both carbon oxides and dehydrated hydroxyapatite. As is already known, hydroxyapatite has two types of water in its structure—adsorbed and lattice water [13]. Adsorbed water is characterized by reversibility and thermal instability from 25 to

Table 3 Structural parameters of the constituent phases of kidney stones

Sample	DTA/°C	Phase	Space group	Constituent phases/wt%	Unit-cell dimensions				Crystallite size/nm
					a/Å	*b*/Å	*c*/Å	*β*/°	
KS1	Before	Whewellite	P12$_1$/c	100	6.2952	14.5967	10.1210	109.45	170
	800	Portlandite	P3m1	99	3.5899	–	4.9160	–	18
		Hydroxyapatite	P$_6$3/m	1	9.3827	–	7.0034	–	35
		Calcite	R3cH	*t.a.*	–	–	–	–	–
		Aragonite	Pmcn	*t.a.*	–	–	–	–	–
	1230	Portlandite	P3m1	97	3.5883	–	4.9149	–	15
		Hydroxyapatite	P63/m	3	9.3757	–	6.9007	–	80
KS2	Before	Whewellite	P12$_1$/c	100	6.2944	14.5933	10.1203	109.12	253
	800	Portlandite	P3m1	45	3.5900	–	4.9228	–	16
		Lime	Fm3m	43	4.8120	–	–	–	156
		Calcite	R3cH	6	4.9804	–	17.1149	–	46
		Vaterite	P6$_3$/mmc	3	4.0992	7.1780	8.3526	–	50
		Hydroxyapatite	P$_6$3/m	3	9.3991	–	6.9013	–	35
	1230	Portlandite	P3m1	18	3.5867	–	4.9324	–	13
		Hydroxyapatite	P$_6$3/m	4	9.3797	–	6.9515	–	80
		Lime	Fm3m	78	4.8110	–	–	–	428
KS3	Before	Whewellite	P12$_1$/c	33	6.2955	14.5965	10.1231	109.46	377
		Weddellite	I4/m	56	12.3539	–	7.3604	–	531
		Hydroxyapatite	P$_6$3/m	11	9.4490	–	6.8917	–	15
	800	Whitlockit	R3cH	45	10.3800	–	37.2016	–	45
		Portlandite	P3m1	44	3.5917	–	4.9158	–	19
		Hydroxyapatit	P$_6$3/m	11	9.4150	–	6.8790	–	35
	1230	Hydroxyapatite	P$_6$3/m	65	9.3939	–	6.8935	–	217
		Whitlockit	R3cH	5	10.4337	–	37.2856	–	80
		Lime	Fm3m	30	4.8113	–	–	–	307

t.a. Trace amount

Table 4 Thermoanalytical data and mass spectroscopy results

Sample	Mass variation/%	Range of variation/°C	Peak/°C	Inorganic fragments
KS1	−12.7	30–315	151	H_2O^+
	−19.6	315–584	470	CO^+, $CO_2{}^+$
	−28.5	584–779	700	$CO_2{}^+$
	−6.7	779–1220	–	–
KS2	−17.7	30–323	150	H_2O^+
	−11.1	323–549	470	CO^+, $CO_2{}^+$
	−36.1	549–884	698	$CO_2{}^+$
	−6.0	884–1220	1019	–
KS3	−8.2	30–313	149	H_2O^+
	−13.6	313–852	468	CO^+, $CO_2{}^+$
	−21.9	582–793	691	$CO_2{}^+$
	−11.2	793–1220	891	–

200 °C. Lattice water is lost reversibly at the temperature of 200–400 °C. The HA dehydration does not occur instantly, but over a wide temperature range. The latter is accompanied with an exothermic process. Third region (~690 °C) is caused by decomposition of calcium carbonate to calcium oxide.

The curves of DTA are differentiated in the area above 800 °C. The samples KS2 and KS3 have endothermic peaks with maximum 1,035 °C (KS2) and 891 °C (KS3), which can be caused by transformation from HA to oxyhydroxyapatite, presented by formula $Ca_{10}(PO_4)_6(OH)_{2-2x}O_xQ_x$. where Q stands for a vacancy [14]. Furthermore, samples undergoing calcinations up to 1,350 °C contain portlandite, $Ca(OH)_2$ (KS1), alternatively lime, CaO (KS3), or their mixture (KS2). All the samples contain different amounts of HA. On increasing of the temperature up to 1,350 °C, the crystallinity of HA increases proportionally to the temperature increment. Thermal analysis, however, revealed the presence of other phases such as polymorphs of calcite ($CaCO_3$)—aragonite and vaterite—in the case of the samples KS1 and KS2, and whitlockite ($Ca_{2.86}Mg_{0.14}(PO_4)_2$) in the sample KS3. Their detection was enabled by the increase of their concentration as a result of the dehydratation and matrix decomposition. Table 3 shows the results of XRD with the constituent phases and lattice parameters, and data of DTA and mass spectroscopy are summarized in Table 4.

Conclusions

This study proposes the structural and thermal properties of three kidney stone samples. The combination of XRD and SEM-EDS microanalysis provides more information about the samples' origins and their compositions. EDS microanalysis identifies trace amounts in homogeneities (P, Cl and Mg) which had not been detected by XRD before thermal analysis. Phosphorus, chlorine, or magnesium was detected by XRD in the form of $Ca_5(PO_4)_3(OH)$, $Ca_5(PO_4)_3(OH, Cl)$—hydroxyapatite and $Ca_{2.86}Mg_{0.14}(PO_4)_2$—whitlockite after thermal analysis.

Thermal analysis showed three characteristic peaks for dehydration and decomposition of calcium oxalates up to 800 °C. Dissimilarity in the curves for the samples KS2 and KS3 above 800 °C is caused by transformation and crystal growth of HA, and by calcination of carbonates. The thermal analysis curves can be also influenced by noncrystalline and organic matrix included in kidney stones.

Acknowledgements This study was supported by the Czech Ministry of Education, Youth and Sports under the project MSM 0021627501.

References

1. Stejskal D. Urolithiaza. Prague: Grada Publishing; 2008.
2. Ansari MS, Gupta NP, Hemal AK, Dogra N, Seth A, Aron M, Sinah TP. Spectrum of stone composition: structural analysis of 1050 upper urinary tract calculi from northern India. Int J Urol. 2005;12:12–6.
3. Kaloustian J, Pauli AM, Pieroni G, Portugal H. The use of thermal analysis in determination of some urinary calculi of calcium oxalate. J Therm Anal Calorim. 2002;70:959–73.
4. Afzal M, Iqbal M, Ahmad H. Thermal analysis of renal stones. J Therm Anal. 1992;38:1671–82.
5. Madhurambal G, Subha R, Mojumdar SC. Crystallization and thermal characterization of calcium hydrogen phosphate dihydrate crystals. J Therm Anal Calorim. 2009;96:73–6.
6. Holager J. Thermogravimetric examination of enamel and dentin. J Dent Res. 1970;49:546–8.
7. Paulik F, Eröss K, Paulik J, Farkas T, Vizkelety T. Investigation of the composition and crystal structure of bone salt by derivatography and infrared spectrophotometry. Hoppe Seyler's Z Physiol Chem. 1969;350:418–26.
8. Mezahi FZ, Oudadesse H, Harabi A, Lucas-Girot A, Le Gal Y, Chaair H, Cathelineau G. Dissolution kinetic and structural behaviour of natural hydroxyapatite vs. thermal treatment. J Therm Anal Calorim. 2009;95:21–9.
9. Mitsionis AI, Vaimakis TC. A calorimetric study of the temperature effect on calcium phosphate precipitation. J Therm Anal Calorim. 2010;99:785–9.
10. Strates B, Georgacopoulou C. Derivatographic thermal analysis of renal tract calculi. Clin Chem. 1969;15:307–11.
11. Ghosh S, Basu S, Chakraborty S, Mukherjee AK. Structural and microstructural characterization of human kidney stones from eastern India using IR spectroscopy, scanning electron microscopy, thermal study and X-ray Rietveld analysis. J Appl Crystallogr. 2009;42:629–35.
12. JCPDS PDF-2 database, release 54. Newton Square, PA, USA: International Centre for Diffraction Data; 2004.
13. LeGeros RY, Bonel G, Legros R. Types of H_2O in human enamel and in precipitated apatites. Calcif Tissue Res. 1987;26:111–8.
14. Liao CJ, Lin FH, Chen KS, Sun JS. Thermal decomposition and reconstruction of hydroxyapatite in air atmosphere. Biomaterials. 1999;20:1807–13.